



Accepted Article

Title: A series of benzylidene linked to hydrazinecarbothioamide as tyrosinase inhibitors
Synthesis, biological evaluation and structure-activity relationship

Authors: Hona Hosseinpoor, Aida Iraj, Najmeh Edraki, Somayeh Pirhadi, Mahshid Attarroshan, Mahsima Khoshneviszadeh, and Mehdi Khoshneviszadeh

This manuscript has been accepted after peer review and appears as an Accepted Article online prior to editing, proofing, and formal publication of the final Version of Record (VoR). This work is currently citable by using the Digital Object Identifier (DOI) given below. The VoR will be published online in Early View as soon as possible and may be different to this Accepted Article as a result of editing. Readers should obtain the VoR from the journal website shown below when it is published to ensure accuracy of information. The authors are responsible for the content of this Accepted Article.

To be cited as: *Chem. Biodiversity* 10.1002/cbdv.202000285

Link to VoR: <https://doi.org/10.1002/cbdv.202000285>

A series of benzylidene linked to hydrazinecarbothioamide as tyrosinase inhibitors**Synthesis, biological evaluation and structure-activity relationship**

Hona Hosseinpoor^{a,b}, Aida Iraj^{b,c}, Najmeh Edraki^b, Somayeh Pirhadi^b, Mahshid Attarroshan^b,
Mahsima Khoshneviszadeh^b, Mehdi Khoshneviszadeh^{a,b*}

^a *Medicinal and Natural Products Chemistry Research Center, Shiraz University of Medical Sciences,
71348 Shiraz, Iran*

^b *Department of Medicinal Chemistry, Faculty of Pharmacy, Shiraz University of Medical Sciences,
71345 Shiraz, Iran*

^c *Central Research Laboratory, Shiraz University of Medical Sciences, 71468 Shiraz, Iran*

***Corresponding author:**

Mehdi Khoshneviszadeh, PharmD, PhD
Medicinal and Natural Products Chemistry Research Center, Shiraz University of Medical Sciences, Shiraz,
Iran
Department of Medicinal Chemistry, Faculty of Pharmacy, Shiraz University of Medical Sciences, Shiraz,
Iran
Tel: +98 713 230 3872; Fax: +98 713 230 2225
E-mail: M.khoshneviszadeh@gmail.com

Abstract

Tyrosinase is a type 3 copper enzyme responsible for skin pigmentation disorders, skin cancer, and enzymatic browning of vegetables and fruits. In the present article, 12 small molecules of benzylidene-hydrazinecarbothioamide were designed, synthesized and evaluated for their anti-tyrosinase activities followed by molecular docking and pharmacophore-based screening. Among synthesized thiosemicarbazone derivatives, **3d** is the strongest inhibitor of mushroom tyrosinase with IC_{50} of 0.05 μ M which demonstrated a 128 fold increase in potency compared to the positive control. Kinetic studies also revealed mix type inhibition by **3d**. Docking studies confirmed the complete fitting of the synthesized compounds into the tyrosinase active site. The results underline the potential of benzylidene hydrazinecarbothioamides as potent pharmacophore to extend the tyrosinase inhibition in drug discovery.

Keywords

Tyrosinase inhibitor, Organic synthesis, Antioxidant assay, Pharmacophore modeling, Molecular docking

Highlight

- 12 derivatives of benzylidene-hydrazinecarbothioamide were designed and synthesized.
- Inhibition of tyrosinase enzyme in the presence of two substrates L-dopa and L-tyrosine were tested.
- **3d** efficiently inhibited tyrosinase with IC_{50} of 0.05 μ M in the in vitro assay.
- Kinetic studies were carried out revealing mix type inhibition by **3d**.
- Additionally, pharmacophore modeling and docking analyses were evaluated.

Introduction

Tyrosinase (TYR) is a binuclear copper oxidoreductase mainly responsible for two catalytic activities. First, in monophenolase action, monophenols such as L-tyrosine hydroxylate to o-diphenolic compound (e.g. L-dopa). Second, during diphenolase activity, o-diphenols oxidizes to o-quinones such as o-dopaquinone. In general, TYR structure is divided into three domains, namely, the central, the N-terminal, and the C-terminal domains. The central domain regarded as the active site of TYR, comprises six histidine residues and two copper ions (Cu_A and Cu_B). Tyrosinase has a critical role in melanogenesis activities responsible for the formation of the color of the skin and hair. However, numerous studies confirmed the role of tyrosinase with some skin pigmentation disorders, skin cancer,^[1] and enzymatic browning of vegetables and fruits.^[2] On the other hand, increase amounts of dopaquinone result in neuronal damage and cell death. It is proposed that tyrosinase is responsible for neurodegenerative disorders.^[3-5] As a result, TYR inhibitors have gained high attention in the therapies of skin pathologies and as well as in dermo-cosmetic treatments and central nervous system (CNS) disorders. Several tyrosinase inhibitors (TYRI) from natural and synthetic origin have been reported in recent years. Different chemical classes of natural compounds from several sources, such as flavonoids,^[6] chalcone, stilbene,^[7] ascorbic acid,^[8] sulphates,^[9] kojic acid, cinnamoyl amide,^[10] tropolone^[7] derivatives have been investigated. Searching for further TYRIs from synthetic source introduced notable example including thiazole,^[11, 12] triazole,^[13] pyrimidine,^[14] benzonitriles,^[15] xanthone,^[16] carbazole.^[17] Among them, tyrosinase inhibitors with the phenolic structure containing hydrazide linker have been characterized by high potency.^[18] It seems that this scaffold could provide new approaches to the discovery of TYRIs.

Therefore, to further find new TYR inhibitors with potential antioxidant activity, in this study, we attempted to connect thiosemicarbazone with the different aryl moieties to design a series of new benzylidenehydrazinecarbothioamide anti-TYR agents.

Results and discussion

Design of novel aryl thiosemicarbazones

L-tyrosine and L-dopa have been regarded as a natural tyrosinase ligand and generally used as tyrosinase pharmacological substrates for the *in vitro* reaction conditions (compound **A** and **B**, Fig1).

We had previously reported 4-hydroxy-N'-methylenebenzohydrazide as small synthetic compounds as a new class of tyrosinase inhibitors, and some of them displayed even better potency than that of kojic acid as a reference. One of the most active derivatives in these series demonstrated an IC₅₀ value of 9.9 μM with competitive-type inhibitory activity (compound **C**, Fig. 1.). Structure-activity relationship (SAR) studies confirmed that all compounds containing the hydrazide linker bounded to 4-hydroxyl of benzyl was active TYRI. The SAR analysis was consistent with the molecular docking study suggesting a crucial role of 4-hydroxyl of benzyl ring *via* H-bound interaction with critical histidine residue.^[19]

Due to the prevalent presence of 4- hydroxyl phenyl motif in tyrosinase natural ligand and even in most of the potent tyrosinase inhibitors, it seems that the presence of substitutions with H-bound interaction ability at *para* position of the benzene ring increases the chance of ligands to reach to the region of tyrosinase active site and improve the inhibitory potency.

Recently, Soares et al reported thiosemicarbazones derivatives (compound **D**, Fig. 1.) as a strong inhibitor of the mushroom tyrosinase. The most active compound in this series exhibited

IC₅₀= 0.35 μM with competitive inhibition. They concluded that the amino groups of the thiosemicarbazone linker can interact *via* hydrogen bonding with the oxygen and nitrogen of Gly170 and Val171 residues.^[20]

- Considering the above mentioned points, the aromatic benzene ring was kept in the structure while substitution patterns at the benzyl ring were evaluated *via* different electron-donating and electron-withdrawing groups with different bulkiness.
- The other structural modification involved the replacement of the aceto hydrazide linker (**C**) with thiosemicarbazide through single bioisosteric modifications while maintaining the linker length constant. From a biological viewpoint, the thio-substituents modified and improved the tyrosinase inhibitory potential and control important metal-chelating function.^[20]
- Based on the previous studies, different derivatives of benzaldehyde thiosemicarbazone demonstrated promising IC₅₀ values that vary from 0.84 to 9 μM.^[21] It seems that phenyl ring with thiosemicarbazone regarded as a very popular scaffold for developing novel tyrosinase inhibitors. As a result, aimed strategies were based on synthesizing new derivatives of thiosemicarbazone and high similarities of designed structure with L-dopa and L-tyrosine, (Fig. 1, **A**, **B**) as the natural ligands of tyrosinase. Besides, for the first time, tyrosinase inhibition in the presence of two substrates was evaluated. It was assumed that the supposed structure reduces the probability of oxidation and increases structural stability.

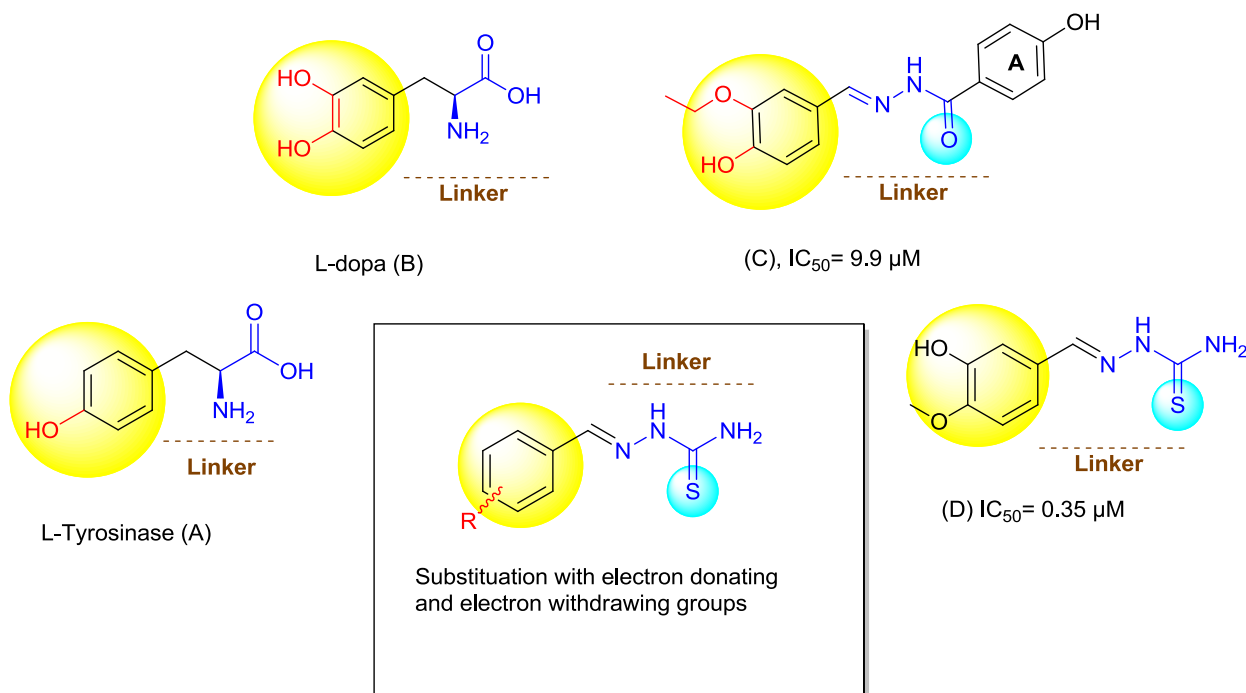
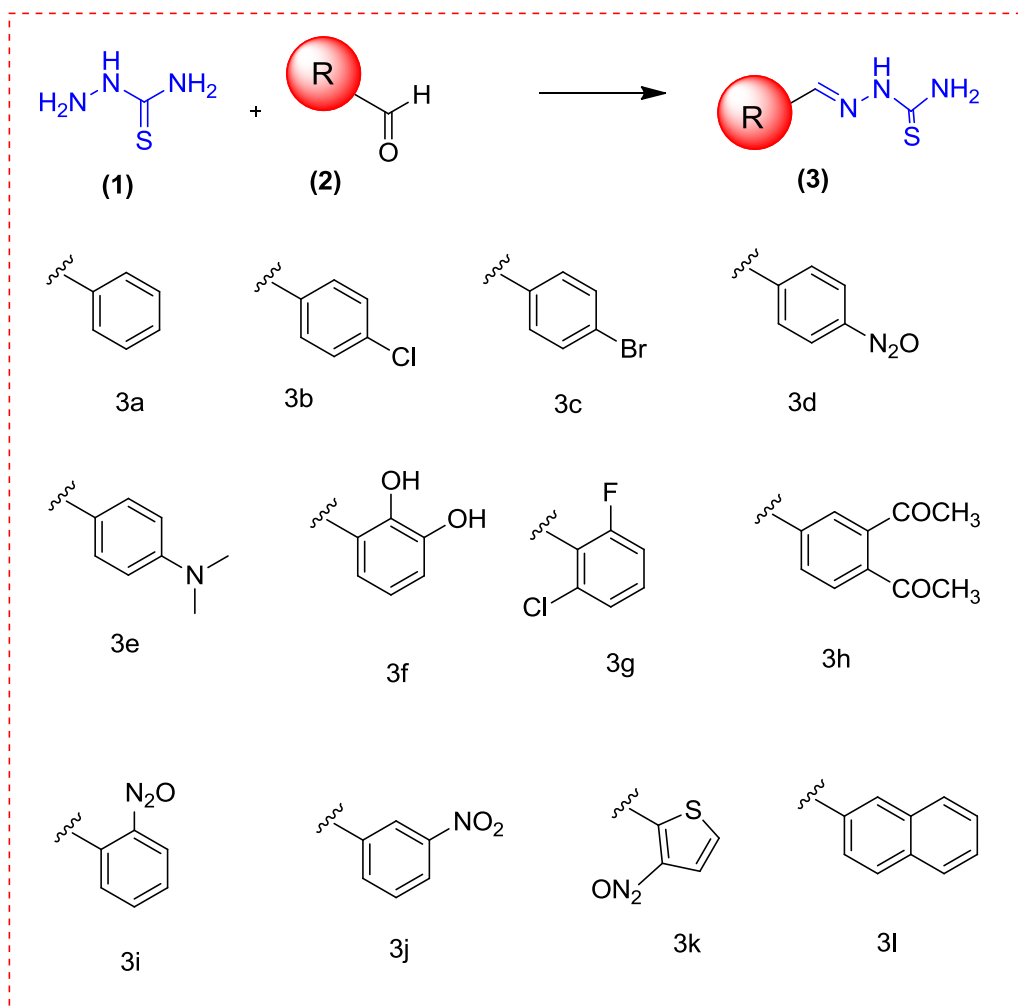


Fig. 1. Rational design and structural modifications of benzylidenehydrazinecarbothioamide scaffold

Chemistry

A series of aryl thiosemicarbazone analogs were synthesized as depicted in Schemes 1.

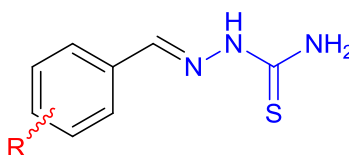


Scheme 1. Synthesis of benzylidenehydrazinecarbothioamide derivatives **3a-l**. Reagents and conditions:
(a) EtOH, reflux, 4 h

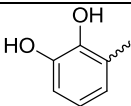
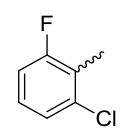
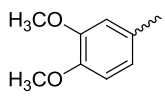
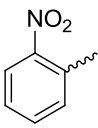
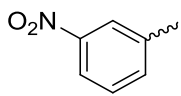
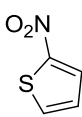
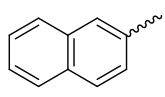
All substituted thiosemicarbazones were prepared by the treatment of thiosemicarbazide with various aldehydes. Briefly, 1 mmol thiosemicarbazide (compound **1**, scheme 1) was reacted with 1 mmol of selected aldehyde in refluxing ethanol to afford desirable compounds.^[22] Completion of the reaction was monitored by TLC. The reaction mixture was cooled. The condensate was filtered and then purified by recrystallization from methanol. Structural determination and signal assignments of the final products **3a-l** (42.63–91.29 %) were accomplished by the application of IR, Mass and NMR experiments. Some of the physical properties of synthesized derivatives are presented in Table 1. The proposed mechanism for this reaction is illustrated in Scheme 2. The

reaction starts by the nucleophilic attack of the lone pair of electrons of the basic nitrogen of the thiosemicarbazides to the carbonyl of different derivatives followed by the elimination of a molecule of water and caused E isomers (confirmed by X-ray crystallography). The electrophilicity of the carbonyl carbon is the main character controlling the yield of the reaction. NO₂ motif induces a strong electron-withdrawing group *via* sigma-bond from the aromatic ring and exerts an inductive electron withdrawal resonance properties. As a result, NO₂ containing compounds showed exceptional reactivity through increasing the positive partial charge on carbon of carbonyl. This information confirmed the high yield of NO₂ containing derivatives.

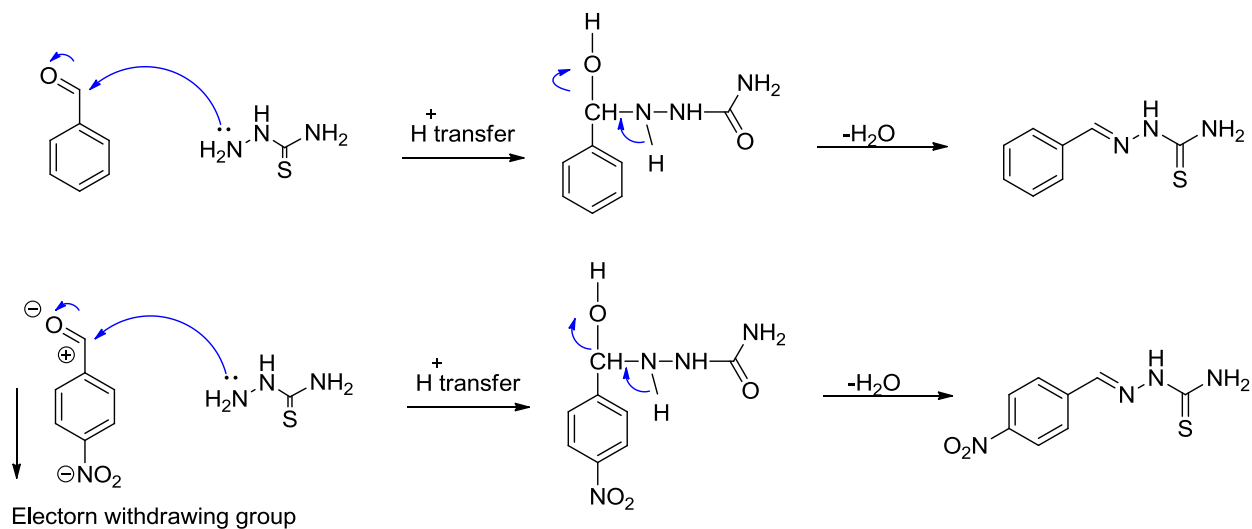
Table 1. Chemical structures and physical properties of the synthesized compounds



Compound	R	Yield (%) ^[a]	Melting point ^[a]
3a		53.4 %	297
3b		48.6 %	332
3c		42.62 %	376
3d		71 %	343
3e		71.62 %	341

3f		90.09 %	331
3g		43.85 %	351
3h		57.94 %	357
3i		91.29 %	343
3j		76.65 %	343
3k		60.17 %	348
3l		68.88 %	348

[a] Yield of isolated purified compounds



Scheme 2. A suggested mechanism for synthesis of benzylidenehydrazinecarbothioamide derivatives

Structure-activity relationship studies

The anti-tyrosinase potential of the synthesized compounds was evaluated by determining IC_{50} values against mushroom tyrosinase. All data of tyrosinase inhibitory activity of benzylidenehydrazinecarbothioamide derivatives with the use of L-dopa and L-tyrosine as substrate are summarized in Table 2 and 3, respectively.

Tyrosinase inhibition with use of L-dopa as a substrate

To find the influence of the type of substitution of the aryl ring on the potency of compounds the SAR analyses have been performed. Based on the observed results, all of the compounds exhibited remarkable anti-tyrosinase activity displaying IC_{50} values in the range of 0.05–17.77 μ M in the case of L-dopa as the substrate and four compounds including **3b**, **3c**, **3d**, and **3j** demonstrated inhibition at submicromolar concentrations.

- The SAR of this set of benzylidenehydrazinecarbothioamide analogs seemed to be very straightforward as the anti-tyrosinase potency was directly correlated to the position of the motif on benzyl ring. Substitutions at the *para* position of benzyl ring (**3b**, **3c**, **3d**, **3e** and **3h**) result in an overall increase in potency with respect to the unsubstituted one. The most potent ligand identified in this study was **3d** (4-nitro, IC_{50} = 0.05 μ M) demonstrated more than 128 fold increase in IC_{50} compared to the positive control. The activity of para analogs changes in the following order: $NO_2 > Br > Cl > N(CH_3)_2$.
- The introduction of halogenated atom into **3a**, resulting in **3b**, **3c** and **3g**. One substituted halogenated derivatives (**3b**, **3c**) exhibited approximately similar potency against tyrosinase cause 30 fold decrease in IC_{50} compared to the unsubstituted one. However,

adding extra halogen atom to the mentioned structure results in significantly drop in the tyrosine inhibitory activity (**3g**, IC_{50} = 5.09 μ M).

- The effects of ring size bonded to thiosemicarbazide were also evaluated. The SAR study indicated that decreasing ring size from six-membered to five units provided **3k** with IC_{50} = 17.77 μ M. While **3l** bearing naphthalene as two fused aromatic moieties demonstrated IC_{50} = 3.38 μ M.

Taking the *in vitro* data together, compound **3d** as the most potent compound was selected to determine the type of inhibition and evaluate *via* molecular dynamic studies.

Table 2. *In vitro* anti-tyrosinase activity of benzylidenehydrazinecarbothioamide analogs in the tyrosinase-catalyzed oxidation of L-dopa

Compounds	% Inhibition at 0.05 μ M ^[a]	% Inhibition at 0.1 μ M ^[a]	% Inhibition at 10 μ M ^[a]	% Inhibition at 50 μ M ^[a]	IC_{50} (μ M) ^[a]
3a	9.7 \pm 4.04	16.7 \pm 3.03	67.71 \pm 0.8	83.85 \pm 1.41	6.4 \pm 1.15
3b	18 \pm 5.98	32.85 \pm 1.5	76.42 \pm 2.76	91.14 \pm 2.62	0.26 \pm 0.38
3c	41.28 \pm 2.22	51.42 \pm 0.1	85.14 \pm 0.8	91.66 \pm 4.44	0.1 \pm 0.56
3d	52.85 \pm 4.44	53.85 \pm 7.07	78.57 \pm 5.25	92.14 \pm 1.01	0.05 \pm 0.64
3e	41.71 \pm 7.03	42.42 \pm 5.5	83.42 \pm 3.23	87.71 \pm 1.21	1.13 \pm 1.35
3f	13.71 \pm 6.06	30.42 \pm 1.2	76.28 \pm 2.62	84.28 \pm 2.01	4.25 \pm 1.27

3g	30.42±1.02	33.85±1.01	69±6.26	84±0.20	5.09±2.04
3h	25.14±1.37	33.57±7.27	73.71±1.21	86.57±1.41	2.182±1.76
3i	21.14±6.46	29.28±3.83	71.57±2.62	85.57±1.81	3.95±1.56
3j	26.85±4.02	45.42±3.9	89.71±0.8	90.57±1.21	0.5±0.94
3k	0	0	44.42±2.4	73.14±4.8	17.77±1.9
3l	5.85±3.03	37.1±6.8	79.71±1.21	85±3.8	3.38±2.16
Kojic acid^[b]					9.28±1.15

^[a] Data presented here are the mean ± S.E.M. of three to five independent experiments

^[b] Standard tyrosinase inhibitor

Tyrosinase inhibition with use of L-tyrosine as the substrate

The *in vitro* anti-tyrosinase activity of the compounds **3a-l** was evaluated using a mushroom tyrosinase in the presence of L-tyrosine as a substrate based on methods already described.

As is obvious in Table 3, the aromatic ring substituents had a significant effect on tyrosinase inhibition. Synthetic derivatives showed IC₅₀ values in the range of 0.027–2.26 μM.

- The strongest inhibitory activity was observed for di-substituted derivatives such as **3h** (3,4-di dimethoxy, IC₅₀=0.027 μM), **3g** (2-chloro-3-fluoro, IC₅₀= 0.046 μM) and **3f** (2,3-hydroxy, IC₅₀= 0.085 μM). It seems that the increase the bulkiness of substituted compound in two different positions of phenyl ring a significantly reduce the IC₅₀. This may be due

to the increasing of occupation of a key pocket within the active site and prevent interaction with the substrate.

- In the case of compounds containing NO₂ motif, surprisingly, the substitution of nitro at the para position of benzyl ring (**3d**) led to a reduction in the potency compare to unsubstituted benzyl. In particular, the order of potency in nitro series was as follows *ortho* > *meta* > *para* which is unlike inhibition in the presence of L-dopa.
- It was interesting to note that benzylidenehydrazinecarbothioamide derivatives showed higher inhibitory activity toward tyrosinase in the presence of L-tyrosine as a substrate compared to L-dopa. In other words, synthetic compounds exhibited much better monophenolase inhibitory potential than diphenolase inhibitory activity.

Table 3. Tyrosinase inhibitory activity of benzylidenehydrazinecarbothioamide in presence of L-tyrosine as substrate

Compounds	% Inhibition				IC ₅₀ (μM) ^[a]
	at 0.05 μM ^[a]	at 0.1 μM ^[a]	at 10 μM ^[a]	at 50 μM ^[a]	
3a	33.87±7.5	39.79±0.6	85.71±0.625	92.71±4.38	0.15±1.05
3b	38.61±3.06	39.38±0.15	73.35±2.16	75.04±2.45	1.011±2.16
3c	19.72±1.59	28.08±6.78	77.73±1.77	89.72±1.45	2.26±0.76
3d	19.52±1.44	19.86±0.67	59.89±7.2	87.56±4.6	1.74±1.64

3e	13.89±4.76	25.09±3.79	78.37±5.05	69.49±6.23	2.26±2.7
3f	23.1±2.1	32.1±5.05	37.7±0.72	95.4±2.73	0.085±2.98
3g	44.1±2.52	47.5±6.13	93.4±1.09	97.5±7.09	0.046±2.09
3h	33.3±4.32	35.7±2.16	87.4±3.5	98.8±0.27	0.027±1.43
3i	37.7±4.32	39.03±2.41	45.1±0.3	88.9±5.05	0.21±0.97
3j	30.67±1.01	33.67±3.13	90.81±0.45	92.00±1.25	0.36±1.37
3k	34.69±8.1	39.59±3.1	77.55±1.56	84.77±1.25	2.23±3.01
3l	36.73±3.1	41.63±3.7	87.75±0.38	88.85±1.73	0.99±1.56
Kojic acid ^[b]					9.28±1.15

^[a] Data presented here are the mean ± S.E.M. of three to five independent experiments

^[b] Standard inhibitor tyrosinase

Kinetic studies of enzyme inhibition

The mechanism of tyrosinase inhibition was investigated by enzyme kinetics, following the similar procedure of the tyrosinase inhibition assay.^[18] Lineweaver-Burk graphics were used to estimate the type of inhibition.^[23-25] Enzyme kinetics was analyzed by recording substrate-velocity curves in the absence and presence of the most potent compound **3d**. Lineweaver-Burk plot introduces the inhibition type as mixed-type, competitive or non-competitive. The graphical analysis of

steady-state inhibition data for compound **3d** is shown in Fig. 2. Therefore, the pattern indicates the inhibition mechanism **3d** is mix-competitive.

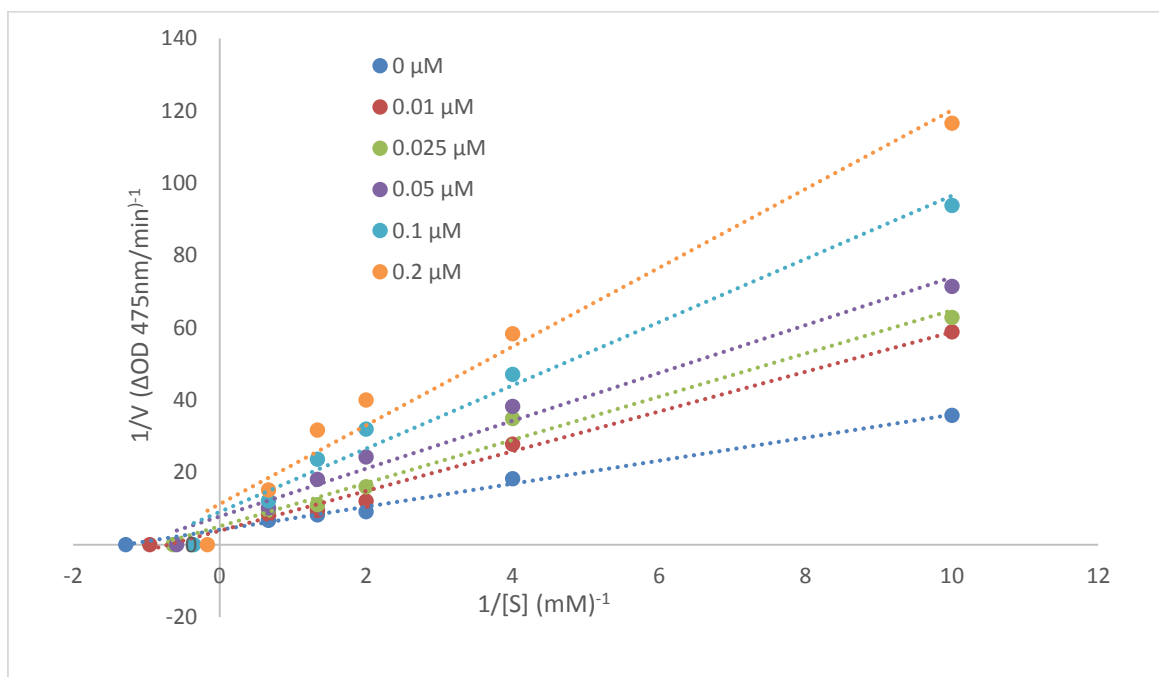


Fig. 2. Lineweaver–Burk plot for the inhibition of mushroom tyrosinase-catalyzed L-dopa oxidation by **3d** at 0.010, 0.025, 0.050, 0.100 and 0.200 μM

DPPH antioxidant assay

In order to evaluate the antioxidant profile of compounds **3e** and **3f** as the most potent compounds, the DPPH[•] scavenging capacity was applied.^[26-28] The IC₅₀ values, that correspond to the concentration of compound that reduces 50% of 2,2-diphenyl-1-picrylhydrazyl (DPPH) radical. Compound **3e** and **3f** displayed a modest dose-dependent antioxidant activity with IC₅₀ of 106.9 and 133.6 μM , respectively. Comparison of this value with data from other studies based on the DPPH assays, it was understood that the presence of the nitro group through their lone pairs of electrons could serve as binding sites in the reaction media to inactivate reactive oxygen and nitrogen species (RONS). Besides, the OH group may giving out active hydrogen to

the free radical to obtain antioxidant properties.^[29, 30] Although tested compounds exhibited weak antioxidant activity compare to that of quercetin as positive control

Table 4. Antioxidant properties of **3e** and **3f** compounds using DPPH assay

Compounds	% Inhibition at 100 μM ^[a]	% Inhibition at 250 μM ^[a]	% Inhibition at 500 μM ^[a]	IC ₅₀ μM ^[a]
3e	47.63±2.2	73.59±2.6	86.11±1.32	106.9±1.8
3f	28.95±0.96	83.81±2.9	93.15±0.35	133.6±0.04
Quercetin ^[b]	-	-	-	4.62±2.26

^[a] Data presented here are the mean \pm S.E.M. of three to five independent experiments

^[b] Positive control

Docking analyses

All scoring functions available in Gold software were investigated in terms of root-mean-square deviation (RMSD) of the redocking process. The only scoring function capable of the generation of an acceptable RMSD was ChemScore. Thus, the docking interaction analysis of all compounds against the tyrosinase enzyme has been done using Gold software using the ChemScore fitness function. The validation process resulted in RMSD 2.0 Å. The ChemScore fitness value of **3d**, (as the most potent compound) and **3k** (the least active compound) plus their interactions with amino acid residues in the tyrosinase active site were tabulated in Table 5. Compound **3d** as the most potent compound in the list, IC₅₀= 0.05 μM , generated the ChemScore value of 32.42. Compound **3k** with IC₅₀ 17.77 μM generated a low score value 21.87 which shows that the scoring function could nearly categorize compounds based on their experimental activities.

Table 5. Docking scores and interactions of compounds against Tyrosinase enzyme

Compound	ChemScore	Interactions
3d	32.42	Hydrogen bonds: Val283 Pi-pi interactions: His263
3k	21.87	Hydrogen bonds: Asn260 Metal acceptor interactions: one Cu ²⁺

3D interaction pattern of compounds **3d**, the best tyrosinase inhibitors in terms of IC₅₀ values, have been shown in Fig. 3a. Compound **3d** showed a pi-pi stacked interaction with His263 via its Nitrobenzene and donated a hydrogen bond in thiourea to residue Val283. The least active compound in the set is compound **3k** with IC₅₀ value 17.77 μM and Chemscore value of 21.87 which is of a low value. 3D interaction pattern of compound **3k** shows two hydrogen bonds with Asn260 from NHs in Thiourea but made the ligand to create a bump with His244 that lowered the binding ability. Although this compound shows a metal acceptor interaction with one of Cu²⁺ ions, it missed pi-pi interaction with His263 as was shown critical in compounds **3d** (Fig 3b).

Overall, it was shown that pi-pi interaction with phenyl ring is critical and potent compounds made it to His263 mostly.

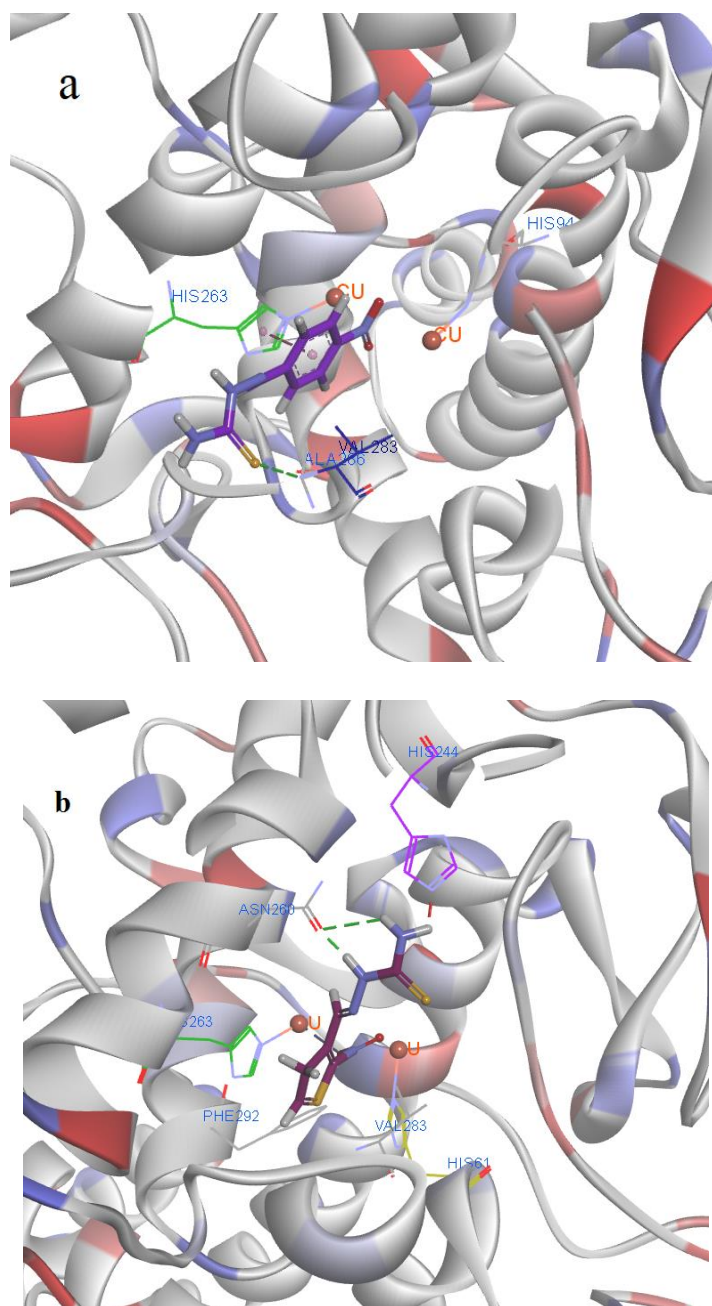


Fig. 3. 3D interaction pattern of compounds **3d** (a) and **3k** (b) in the active site of TYR enzyme

Pharmacophore modeling

A set of pharmacophore models has been developed and the best constructed model 1 generated a score value of 33.68. All the input compounds could map all the features, as these compounds

share a common substructure. Model 1 contained 4 features including 2 hydrogen bond donor, one acceptor and one aromatic features, see Fig. 4. One aromatic feature overlapped aromatic ring of benzoic acid in compound **3d** and one hydrogen bond acceptor feature covered sulfur in thiourea. Docking interaction analyses has shown that compounds **3d**, **3b**, **3c**, **3l**, **3d**, **3e** and **3f** accepted hydrogen bonds via sulfur in thiourea from Val283, or Arg268. Aromatic ring of phenyl contributed in important interaction of pi-pi with His263 and was seen in all compounds except for **3k** and in compound **3l** was seen with Ser282. Both two hydrogen bond donor features, overlapped two NH groups in thiourea. Amino groups in thiourea donated hydrogen bonds to Asn260 in compounds **3f**, **3i** and to Gly281 in compounds **3a**, **3g**, and **3h**.

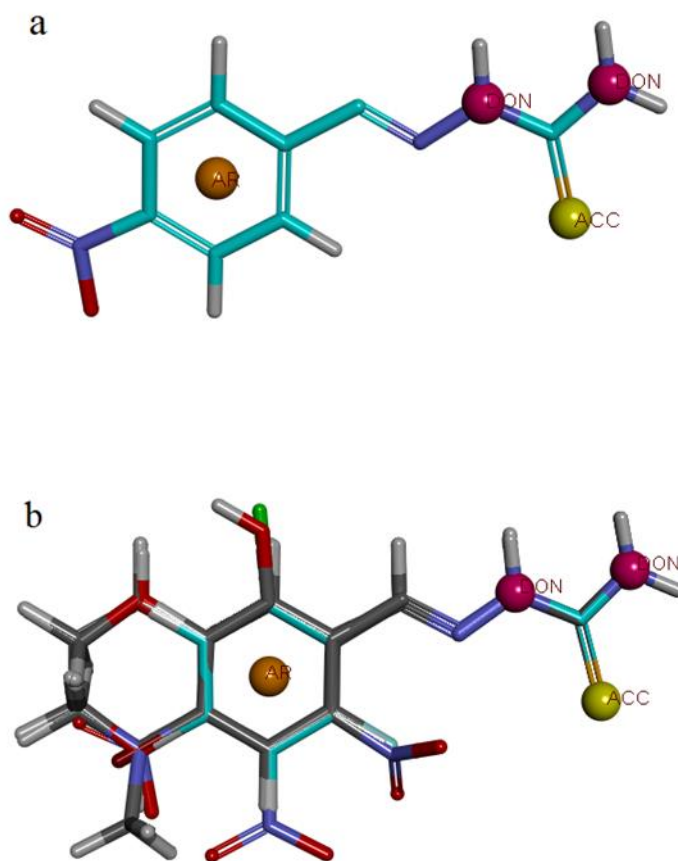


Fig. 4. Pharmacophore model 1 aligned on compound **3d**. (a) AR: Aromatic feature, DON: Hydrogen bond donor feature, ACC: hydrogen bond acceptor feature. (b) All compounds except **3k** aligned on model 1 (b).

Conclusion

Following our expertise in the rational design of tyrosinase inhibitor, herein, we designed, synthesized and evaluated highly potent tyrosinase inhibitors from the thiosemicarbazide family. Most compounds exhibited pronounced anti-tyrosinase activity compare the reference compound kojic acid, with IC_{50} values in the range of 0.05–17.77 μ M for L-dopa as substrate and 0.027–2.26 μ M in the presence of L-tyrosine. It is important to note that all of these compounds, due to the presence of hydrazinecarboxamide on the phenyl ring, have a high affinity for tyrosine enzyme. Molecular docking study of **3d** into TYR revealed that this molecule completely embedded into the TYR pocket and showed a pi-pi stacked interaction with His263 *via* its benzyl pendant. Besides the additional hydrogen binding interactions with Val283 were also observed. Pharmacological results proved that the aryl thiosemicarbazone is a privileged scaffold or even fragment for the design and discovery of novel anti-tyrosinase.

Material and method

Chemistry

All reagents were reagent grade quality and obtained from Sigma-Aldrich (Prague, Czech Republic). The reaction process was monitored using thin-layer chromatography on the glass-backed silica gel sheets (Silica Gel 60 GF254) and visualized under UV light (254 nm). Column chromatography was performed on silica gel (90–150 mm; Merck Chemical Inc.). 1H and ^{13}C NMR spectra were determined by a Bruker FT-300 MHz spectrometer in $DMSO-d_6$. All the chemical shifts were reported as (δ) values (ppm). Mass spectra were obtained on the Agilent

7890A spectrometer at 70 eV. The infrared (IR) spectra were run as KBr disk on Perki-Elmer Spectrum RXI FTIR.

Procedure for the synthesis of thiosemicarbazones derivatives (3a-l)

All substituted thiosemicarbazones were prepared by treatment of thiosemicarbazid with various benzaldehydes. Briefly, 1mmol thiosemicarbazide was added to 1mmol respective substituted benzaldehyde. The reaction mixture was stirred at room temperature for 2 h followed by refluxing for 6 h. The progress of reaction is monitored by TLC. After cooling, the solvent was evaporated under reduced pressure and the formed precipitate was recrystallized from methanol.

Synthesis of (E)-1-benzylidenethiosemicarbazide (3a)

White powder; yield: 53.4%; ^1H NMR (DMSO- d_6 , 300 MHz) δ_{H} (ppm): 11.46 (s, 1H, NH), 8.22 (s, 1H, N=CH), 8.05 (brs, 1H, NH₂), 8.01 (brs, 1H, NH₂), 7.77-7.79 (m, 2H, phenyl-C_{2,6}-H), 7.39-7.40 (m, 3H, phenyl C_{3,4,5}-H); ^{13}C NMR (DMSO- d_6 , 125 MHz): δ_{C} (ppm): 178.4 (C=S), 142.7 (HC=N), 134.6 (C₁), 130.2 (C₄), 129.1 (C₃,C₅), 127.7 (C₂,C₆); MS (EI), m/z (%): 179.1 (M⁺, 100), 162 (10), 119.1 (55.5), 104.1 (63.8), 93 (27.7), 76 (63.3), 60 (50), 43 (77.7); IR (KBr) ν (cm⁻¹): 3468.9 (NH₂), 3394.08 (NH), 3145.40 (=CH stretch), 1582.9, 1601.13 (C=C aromatic), 1326(C-N), 1159.50 (C=S stretch).

Synthesis of (E)-1-(4-chlorobenzylidene)thiosemicarbazide (3b)

White powder; yield: 48.6%; ^1H NMR (DMSO- d_6 , 300 MHz) δ_{H} (ppm): 11.50 (s, 1H, NH), 8.26 (s, 1H, HC=N), 8.09 (brs, 1H, NH₂), 8.02 (brs, 1H, NH₂), 7.44-7.46 (m, 2H, phenyl-C_{2,6}-H), 7.82-7.86 (m, 2H, phenyl-C_{3,5}-H); ^{13}C NMR (DMSO- d_6 , 125 MHz): δ_{C} (ppm): 178.5 (C=S), 141.2 (HC=N), 133.9 (C₄), 132 (C₁), 129.6 (C_{3,5}), 123.4 (C_{2,6}); MS (EI), m/z (%): 213.1 (M⁺, 84.6), 196

(11.5), 153.1 (34.6), 138 (57.6), 111 (38.4), 89 (42.3), 76 (80.7), 60 (57.6), 43 (100); IR(KBr) ν (cm^{-1}): 3165.3, 3280.57 (NH_2), 3437.56 (NH), 1525, 1600.7 (C=C), 1282.8 (C-N), 1090.5 (aryl chloride), 1016.9 (C=S).

Synthesis of (E)-1-(4-bromobenzylidene)thiosemicarbazide (3c)

White powder; yield: 42.62%; ^1H NMR (DMSO- d_6 , 300 MHz) δ_{H} (ppm): 11.50 (s, 1H, NH), 8.26 (s, 1H, HC=N), 8.09 (brs, 1H, NH_2), 8.00 (brs, 1H, NH_2), 7.75-7.78 (m, 2H, phenyl- $\text{C}_{3,5}$ -H), 7.57-7.6 (m, 2H, phenyl- $\text{C}_{2,6}$ -H); ^{13}C NMR (DMSO- d_6 , 125 MHz): δ_{C} (ppm): 178.5 (C=S), 141.3 (HC=N), 133.9 (C_4), 132.0 (C_1), 129.6 ($\text{C}_{3,5}$), 123.4 ($\text{C}_{2,6}$); MS (EI), m/z (%): 259 ((M+2) $^+$, 87.5), 257 (M $^+$, 87), 199 (18.7), 184 (40.6), 157 (21.8), 118 (50), 102 (28.1), 76 (90.6), 60 (84.3), 43 (100); IR (KBr) ν (cm^{-1}): 3165.9, 3287 (NH_2), 3436.2 (NH), 1523.5, 1600.8 (C=C), 1286 (C-N), 1089 (C=S).

Synthesis of (E)-1-(4-nitrobenzylidene)thiosemicarbazide (3d)

Yellow powder; yield: 71 %; ^1H NMR (DMSO- d_6 , 300 MHz) δ_{H} (ppm): 11.72 (s, 1H, NH), 8.42 (s, 1H, HC=N), 8.26 (brs, 1H, NH_2), 8.18 (brs, 1H, NH_2), 8.06-8.08 (m, 4H, phenyl- $\text{C}_{2,3,5,6}$ -H); ^{13}C NMR (DMSO- d_6 , 125 MHz): δ_{C} (ppm): 178.9 (C=S), 147.9 (HC=N), 141.1 (C_4), 139.9 (C_1), 128.5 ($\text{C}_{3,5}$), 124.2 ($\text{C}_{2,6}$); MS (EI), m/z (%): 224 (M $^+$, 65.6), 165 (11.25), 149 (12.5), 135 (15.6), 118 (25), 102 (18.7), 89 (21.8), 76 (81.2), 60 (62.5), 43 (100); IR (KBr) ν (cm^{-1}): 3092.7, 3142.1 (NH_2), 3491.2 (NH), 1588.7, 1578.1 (C=C), 1338.6, 1525 (NO_2), 1288.1 (C=N), 1097.8 (C=S).

Synthesis of (E)-1-(4-nitrobenzylidene)thiosemicarbazide (3e)

Pale yellow powder; yield: 71.62%; ^1H NMR (DMSO- d_6 , 300 MHz) δ_{H} (ppm): 11.195 (s, 1H, NH), 8.01 (s, 1H, HC=N), 7.93 (brs, 1H, NH_2), 7.77 (brs, 1H, NH_2), 7.56-7.59 (m, 2H, phenyl-

C_{3,5}-H), 6.67-6.70 (m, 2H, phenyl-C_{2,6}-H), 2.95 (s, 6H, 2CH₃); ¹³C NMR (DMSO-*d*₆, 125 MHz): δ_c (ppm)= 177.4 (C=S), 151.8 (HC=N), 143.8 (C₁), 129.0 (C₄), 121.8 (C_{2,6}), 112.1 (C_{3,5}), 40.6 (2CH₃); MS (EI), m/z (%): 222 (M⁺, 90), 205 (87.5), 188 (50), 162 (27.5), 147 (100), 118 (25), 91 (30), 60 (28.7), 43 (30); IR (KBr) ν (cm⁻¹): 3249, 3147.9 (NH₂), 3404 (NH), 1553, 1589 (C=C), 1358.4 (C-N aromatic tertiary amine), 1056.2 (C-N), 1184.2 (C=S).

Synthesis of (E)-1-(2,3-dihydroxybenzylidene)thiosemicarbazide (3f)

Gray powder, yield: 90.09%; MS (EI), m/z (%): ¹H NMR (DMSO-*d*₆, 300 MHz) δ_H (ppm): 11.40 (s, 1H, NH), 9.69 (s, 1H, HC=N), 8.96 (brs, 1H, NH₂), 8.37 (brs, 1H, NH₂), 6.61-7.3 (m, 3H, phenyl-C_{4,5,6}-H), 7.36 (s, 1H, OH-C₂), 7.87 (s, 1H, OH-C₃); ¹³C NMR (DMSO-*d*₆, 125 MHz): δ_c (ppm)= 177.9 (C=S), 145.6 (HC=N), 141.16 (C₂), 141.12 (C₃), 121.2 (C₁), 119.6 (C₄), 117.6 (C₆), 116.0 (C₅); 211 (M⁺, 90), 162 (18.1), 120 (100), 92 (22.7), 65 (16.3), 43 (9); IR (KBr) ν (cm⁻¹): 3357.6 (NH₂), 3461 (NH), 3254.1 (OH), 1234.4 (C-O), 1614, 1697 (C=C), 1221 (C=S).

Synthesis of (E)-1-(2-chloro-6-fluorobenzylidene)thiosemicarbazide (3g)

White powder; yield: 43.85%; ¹H NMR (DMSO-*d*₆, 300 MHz) δ_H (ppm): 11.79 (s, 1H, NH), 8.48 (brs, 1H, NH₂), 8.36 (brs, 1H, NH₂), 7.37-7.44 (m, 3H, phenyl-C_{3,4,5}-H), 7.34 (s, 1H, HC=N); ¹³C NMR (DMSO-*d*₆, 125 MHz): δ_c (ppm)= 178.8 (C=S), 135.9 (HC=N), 126.7 (C₆), 126.6 (C₂), 120.8 (C₅), 120.6 (C₃), 116 (C₁), 115.7 (C₄); MS (EI), m/z (%): 231 (M⁺, 56.2), 156 (37.5), 137 (40.6), 107 (50), 76 (72.8), 60 (62.5), 43 (100); IR(KBr) ν (cm⁻¹): 3146.5 (NH₂), 3408 (NH), 1597, 1538 (C=C), 1239 (C=S), 1286 (C-N), 1167 (Ar-F), 1094 (Ar-Cl).

Synthesis of (E)-1-(3,4-dimethoxybenzylidene)thiosemicarbazide (3h)

White powder; yield: 57.94%; ^1H NMR (DMSO- d_6 , 300 MHz) δ_{H} (ppm): 11.34 (s, 1H, NH), 8.18 (s, 1H, HC=N), 8.04 (brs, 1H, NH₂), 7.97 (brs, 1H, NH₂), 7.52 (s, 1H, phenyl-C₂-H), 7.13 (d, J = 8.4 Hz, 1H, phenyl-C₆-H), 6.94 (d, J = 8.4 Hz, 1H, phenyl-C₅-H), 3.81 (s, 3H, OCH₃), 3.77 (s, 3H, OCH₃); ^{13}C NMR (DMSO- d_6 , 125 MHz): δ_{C} (ppm)= 177.9 (C=S), 151.0 (HC=N), 149.5 (C₃), 143.0 (C₄), 127.3 (C₂), 122.6 (C₅), 111.6 (C₁), 108.9 (C₆), 55.9 (CH₃), 56.1 (CH₃); MS (EI), m/z (%): 239 (M⁺, 88.4), 222 (88.4), 168 (100), 137 (42.3), 119 (44.2), 92 (57.6), 77 (61.5), 60 (50), 43 (76.9); IR (KBr) $\nu(\text{cm}^{-1})$: 3117.1, 3182 (NH₂), 3351 (NH), 1536, 1618 (C=C), 1146 (Ar-O-C), 1018 (C-N).

Synthesis of (E)-1-(2-nitrobenzylidene)thiosemicarbazide (3i)

Yellow powder; yield: 91.29%; ^1H NMR (DMSO- d_6 , 300 MHz) δ_{H} (ppm): 11.75 (s, 1H, NH), 8.46 (s, 1H, HC=N), 8.44 (brs, 1H, NH₂), 8.42 (brs, 1H, NH₂), 8.14 (d, J = 8.4 Hz, 1H, phenyl-C₆-H), 8.02 (d, J = 8.4 Hz, 1H, phenyl-C₃-H), 7.73 (t, J = 7.8 Hz, 1H, phenyl-C₅-H), 7.61 (t, J = 7.8 Hz, 1H, phenyl-C₄-H); ^{13}C NMR (DMSO- d_6 , 125 MHz): δ_{C} (ppm)= 178.8 (C=S), 143.7 (HC=N), 137.6 (C₂), 133.7 (C₁), 130.7 (C₃), 128.8 (C₄), 128.7 (C₆), 124.9 (C₅); MS (EI), m/z (%): 224 (M⁺, 28.5), 207 (53.5), 188 (89.2), 167 (10.7), 149 (28.5), 120 (21.4), 91 (42.8), 76 (71), 60 (71.4), 43 (100); IR (KBr) $\nu(\text{cm}^{-1})$: 3114 (NH₂), 3365 (NH), 1432, 1606 (C=C), 1231 (C=S), 1101 (C-N), 1333, 1542 (NO₂).

Synthesis of (E)-1-(3-nitrobenzylidene)thiosemicarbazide (3j)

White powder; yield: 76.65%; ^1H NMR (DMSO- d_6 , 300 MHz) δ_{H} (ppm): 11.64 (s, 1H, NH), 8.65 (s, 1H, phenyl-C₂-H), 8.35 (brs, 1H, NH₂), 8.33 (brs, 1H, NH₂), 8.22-8.26 (m, phenyl-C₆-H), 8.16-8.21 (m, 1H, phenyl-C₄-H), 8.13 (brs, 1H, HC=N), 7.67 (t, J = 8.0 Hz, 1H, phenyl-C₅-H); ^{13}C NMR (DMSO- d_6 , 125 MHz): δ_{C} (ppm)= 178.7 (C=S), 148.8 (HC=N), 140.3 (C₃), 136.6 (C₂), 134.0

(C₄), 130.5 (C₁), 124.3 (C₅), 121.8 (C₆); MS (EI), m/z (%): 224 (M⁺, 25), 207 (57.1), 188 (92.8), 149 (28.5), 120 (20), 105 (21.4), 76 (71.4), 60 (71.4), 43 (100); IR (KBr) ν (cm⁻¹): 3114 (NH₂), 3365 (NH), 1432, 1606 (C=C), 1231 (C=S), 1101 (C-N), 1333, 1542 (NO₂).

Synthesis of (E)-1-((2-nitrothiophen-3-yl)methylene)thiosemicarbazide (3k)

Orange powder; yield: 60.17%; ¹H NMR (DMSO-*d*₆, 300 MHz) δ _H (ppm): 11.82 (s, 1H, NH), 8.63 (brs, 1H, NH₂), 8.31 (brs, 1H, NH₂), 8.04-8.31 (m, 2H, C=C), 7.50 (s, 1H, HC=N); ¹³C NMR (DMSO-*d*₆, 125 MHz): δ _C (ppm)= 178.6 (C=S), 151.1 (HC=N), 147.1 (C₂), 135.7 (C₃), 130.8 (C₁), 129.6 (C₄); m/z (%): 147 (10), 120 (100), 92 (36.6), 65 (30), 43 (16.6); IR (KBr) ν (cm⁻¹): 3025, 2985 (NH₂), 3395 (NH), 1525, 1603 (C=C), 1106 (C=S), 1348 (C-N), 844 (thiophen ring).

Synthesis of (E)-1-((naphthalen-2-yl)methylene)thiosemicarbazide (3l)

White powder; yield: 68.88 %; 11.56 (s, 1H, NH), 8.28 (brs, 1H, NH₂), 8.22 (s, 1H, HC=N), 8.13 (brs, 1H, NH₂), 8.17 (d, *J* = 8.4 Hz, 1H, phenyl-C₄-H), 8.11 (s, 1H, phenyl-C₂-H), 7.89-7.93 (m, 3H, phenyl-C_{5,6,7}-H), 7.52-7.55 (m, 2H, phenyl-C_{9,10}-H); ¹³C NMR (DMSO-*d*₆, 125 MHz): δ _C (ppm)= 178.4 (C=S), 142.7 (HC=N), 134 (C₁), 133.3 (C₂), 132.4 (C₁₀), 129.4 (C₉), 129.3 (C₃), 128.6 (C₈), 128.1 (C₄), 127.4 (C₇), 127.1 (C₅), 123.5 (C₆); MS (EI), m/z (%): 229 (M⁺, 77.7), 158 (100), 139 (38.8), 127 (50), 115 (38.8), 76 (22.2), 60 (27.7), 43 (27.7); IR (KBr) ν (cm⁻¹): 3245 (NH₂), 3380 (NH), 1599, 1540 (C=C).

Tyrosinase inhibition assay

The tyrosinase activity was performed by assay of monophenolase and diphenolase activity. L-dopa is a substrate for diphenolase assay activity and L-Tyr is a substrate for monophenolase assay activity, At first 160 μ L phosphate buffer (50 mM, pH= 6.8) was added to each well except blank (190 μ L) and then 10 μ L tyrosinase (5771 units/mg solid) (0.5 mg/mL) was added to all wells and

afterwards inhibitors were added accordance to protocol and finally 10 μL kojic acid as negative control and 10 μL DMSO as positive control were added. In second step the plate was incubated for 20 min. In third step 20 μL L-dopa and L-tyr considering to related test was added. In L-dopa test the absorbance immediately was read for 1min in 475 nm. But in L-Tyr test after adding substrate the plate was incubated for 10min and then the absorbance was read. The IC_{50} was calculated by CurveExpert v1.3, The IC_{50} values are presented in table 2 and 3.

Kinetic assay

The kinetic study was determined by Lineweaver-Burk plot analysis (Fig. 2.) and it was carried out on several concentrations of **3d** compound and L-dopa as the substrate. Pre-incubation and measurement time was the same as discussed in the mushroom tyrosinase inhibition assay protocol. Considering to relation of $1/V = 1/[S] K_m/V_m + 1/V_m$ and line equation, the Michaelis constant (K_m) and the maximal velocity (V_{max}) of the tyrosinase activity were determined at various concentrations of L-dopa (0.1, 0.25, 0.5, 0.75 and 1.5 mM) as a substrate. The inhibition type of the enzyme was assayed by Line weaver Burk plots of the inverse of velocities ($1/V$) versus the inverse of substrate concentrations $1/[S]$ mM.^[31-33]

Free radical scavenging activity

The antioxidant activity of purified compounds was measured by the DPPH method.^[34-36] 20 μL of different concentration of drugs (500, 250, 100 μM) were added to 180 μL of 110 μM of metanolic solution of DPPH in 96 well plate. The mixture was shaken vigorously for 20 min at room temperature under sodium light. The absorbance was determined at 517 nm and the percentage of activity was calculated. Quercetin was used as positive control and methanol as the negative control. The DPPH scavenging effect was calculated as follows:

$$\text{Scavenging effect (\%)} = \frac{(A_0 - A_1)}{A_0} \times 100$$

Where A0 is the absorbance of the control, and A1 is the absorbance in the presence of the sample. All determinations were performed in triplicate. All tests were undertaken on three replicates and the results were averaged and compared with the quercetin as standard.^[30]

Molecular docking

All compounds were sketched using MarvinSketch 18.20.0 and energy minimized by Open Babel 2.4.0 using the steepest descent algorithm. GOLD docking program was used for doing docking analyses. X-ray crystal structure of *Agaricus bisporus* tyrosinase including tropolone as the native ligand in the binding site with PDB code of 2Y9X was applied for doing docking analyses. The binding site of the tyrosinase comprises Cu²⁺ metal ions which all were regarded for docking. Enzyme structure was prepared using Discovery studio client in such a way that all hydrogens were added and all ligands were removed. The binding site of the enzyme for the docking was defined automatically using the coordinates of the native ligand tropolone in such a way that 8 Å around the ligand was defined as the binding site. In order to run docking analyses for all compounds, we tried all available scoring functions in GOLD namely CHEMPLP, ChemScore, ASP, and GoldScore. To choose and validate the docking algorithm, tropolone inside the 2Y9X was redocked using all mentioned scoring functions.^[37-39]

Pharmacophore model building

All structures except for **3k** with IC₅₀ value 17.77 μM were collected as a multi mol file and fed to PharmaGist server for pharmacophore model building. PharmaGist is a free web server for detection of pharmacophores which are the spatial arrangement of features that enable a molecule

to interact with a specific target receptor. The highest-scoring pharmacophores were defined by multiple flexible alignments of the input inhibitors.^[40]

The list of abbreviations

L-Tyr: L-tyrosinase, L-dopa: L-dihydroxyphenylalanine, Val: Valine, Gly: Glycine, Glu: Glutamic acid, Ala: Alanine, Asn: Asparagine, Arg: Arginine, His: Histidine, LGA: Lamarckian genetic algorithm, DMSO-d₆: deuterated dimethyl sulfoxide, ¹H NMR: proton nuclear magnetic resonance; ¹³C NMR: carbon-13 nuclear magnetic resonance, TYR: Tyrosinase, CNS: Central nervous system, DPPH: 2,2-diphenyl-1-picrylhydrazyl, RMSD: Root-mean-square deviation.

Declarations

Availability of data and materials

The datasets used and analyzed during the current study are available from the corresponding author on reasonable request. We have presented all data in the form of tables and figures.

Competing interests

The authors declare that they have no competing interests.

Funding

The authors wish to thank the support of the Vice-Chancellor for Research of Shiraz University of Medical Sciences. This study was part of the Ph.D. thesis of Hona Hosseinpour. This agency was not involved in the design of the study and collection, analysis, and interpretation of data as well as in writing the manuscript.

Authors' contributions

Me.K conceived the research idea. AI, Ma.K and H.H conducted the experiments, performed synthesise and biological tests, analyzed the data in addition to preparing the first draft. N.E, Me.K and RM analyzed and interpreted the data and provided technical guidance. S.P performed the docking study. H.H, AI, RM,

N.E and Me.K critically read and revised the paper. All authors read and approved the final manuscript.

Me.K supervised all phases of the study.

Corresponding author

Correspondence to Mehdi Khoshneviszadeh.

Reference

- [1] V. Del Marmol, F. Beermann, 'Tyrosinase and related proteins in mammalian pigmentation', *FEBS Lett.* **1996**, *381*, 165-168.
- [2] O. Nerya, R. Ben-Arie, T. Luzzatto, R. Musa, S. Khativ, J. Vaya, 'Prevention of Agaricus bisporus postharvest browning with tyrosinase inhibitors', *Postharvest Biol. Technol.* **2006**, *39*, 272-277.
- [3] T. Hasegawa, 'Tyrosinase-expressing neuronal cell line as in vitro model of Parkinson's disease', *Int. J. Mol. Sci.* **2010**, *11*, 1082-1089.
- [4] E. Greggio, E. Bergantino, D. Carter, R. Ahmad, G. E. Costin, V. J. Hearing, J. Clarimon, A. Singleton, J. Eerola, O. Hellström, 'Tyrosinase exacerbates dopamine toxicity but is not genetically associated with Parkinson's disease', *J. Neurochem.* **2005**, *93*, 246-256.
- [5] E. Neagu, G. Paun, C. Albu, G.-L. Radu, 'Assessment of acetylcholinesterase and tyrosinase inhibitory and antioxidant activity of Alchemilla vulgaris and Filipendula ulmaria extracts', *J. Taiwan Inst. Chem. Eng.* **2015**, *52*, 1-6.
- [6] Y. J. Kim, 'Rhamnetin attenuates melanogenesis by suppressing oxidative stress and pro-inflammatory mediators', *Biol. Pharm. Bull.* **2013**, b13-00276.
- [7] W. T. Ismaya, H. J. Rozeboom, A. Weijn, J. J. Mes, F. Fusetti, H. J. Wichers, B. W. Dijkstra, 'Crystal structure of Agaricus bisporus mushroom tyrosinase: identity of the tetramer subunits and interaction with tropolone', *Biochemistry* **2011**, *50*, 5477-5486.
- [8] Y. Yuan, W. Jin, Y. Nazir, C. Fercher, M. A. T. Blaskovich, M. A. Cooper, R. T. Barnard, Z. M. Ziora, 'Tyrosinase inhibitors as potential antibacterial agents', *Eur. J. Med. Chem.* **2019**, 111892.
- [9] E. W. C. Chan, Y. Y. Lim, L. Wong, F. S. Lianto, S. Wong, K. Lim, C. Joe, T. Lim, 'Antioxidant and tyrosinase inhibition properties of leaves and rhizomes of ginger species', *Food Chem.* **2008**, *109*, 477-483.
- [10] L. Georgiev, M. Chochkova, I. Totseva, K. Seizova, E. Marinova, G. Ivanova, M. Ninova, H. Najdenski, T. Milkova, 'Anti-tyrosinase, antioxidant and antimicrobial activities of hydroxycinnamoylamides', *Med. Chem. Res.* **2013**, *22*, 4173-4182.
- [11] K. Piechowska, M. Switalska, J. Cytarska, K. Jaroch, K. Luczykowski, J. Chalupka, J. Wietrzyk, K. Misiura, B. Bojko, S. Kruszewski, K. Z. Laczkowski, 'Discovery of tropinone-thiazole derivatives as potent caspase 3/7 activators, and noncompetitive tyrosinase inhibitors with high antiproliferative activity: Rational design, one-pot tricomponent synthesis, and lipophilicity determination', *Eur J Med Chem* **2019**, *175*, 162-171.
- [12] R. S. Ismail, N. S. Ismail, S. Abuserii, D. A. A. El Ella, 'Recent advances in 4-aminoquinazoline based scaffold derivatives targeting EGFR kinases as anticancer agents', *Future J. Pharm. Sci* **2016**, *2*, 9-19.
- [13] M. B. Tehrani, P. Emani, Z. Rezaei, M. Khoshneviszadeh, M. Ebrahimi, N. Edraki, M. Mahdavi, B. Larijani, S. Ranjbar, A. Foroumadi, M. Khoshneviszadeh, 'Phthalimide-1,2,3-triazole hybrid compounds as tyrosinase inhibitors; synthesis, biological evaluation and molecular docking analysis', *J. Mol. Struct.* **2019**, *1176*, 86-93.

- [14] S. S. Mirmortazavi, M. Farvandi, H. Ghafouri, A. Mohammadi, M. Shourian, 'Evaluation of novel pyrimidine derivatives as a new class of mushroom tyrosinase inhibitor', *Drug Des., Dev. Ther.* **2019**, *13*, 2169-2178.
- [15] K.-i. Nihei, I. Kubo, 'Benzonitriles as tyrosinase inhibitors with hyperbolic inhibition manner', *Int. J. Biol. Macromol.* **2019**, *133*, 929-932.
- [16] L. Yu, L. Chen, G. Luo, L. Luo, W. Zhu, P. Yan, P. Zhang, C. Zhang, W. Wu, 'Study on synthesis and biological evaluation of 3-aryl substituted xanthone derivatives as novel and potent tyrosinase inhibitors', *Chem. Pharm. Bull.* **2019**, c19-00572.
- [17] U. Ghani, 'Carbazole and hydrazone derivatives as new competitive inhibitors of tyrosinase: Experimental clues to binuclear copper active site binding', *Bioorg. Chem.* **2019**, *83*, 235-241.
- [18] A. Iraj, T. Adelpour, N. Edraki, M. Khoshneviszadeh, R. Miri, M. Khoshneviszadeh, 'Synthesis, biological evaluation and molecular docking analysis of vaniline-benzylidenehydrazine hybrids as potent tyrosinase inhibitors', *BMC Chem.* **2020**, *14*, 28.
- [19] A. Iraj, M. Khoshneviszadeh, P. Bakhshizadeh, N. Edraki, M. Khoshneviszadeh, 'Structure-Based Design, Synthesis, Biological Evaluation and Molecular Docking Study of 4-Hydroxy-N'-methylenebenzohydrazide Derivatives Acting as Tyrosinase Inhibitors as Potentiate Anti-Melanogenesis Activities', *Medicinal chemistry (Sharīqah (United Arab Emirates))* **2019**.
- [20] M. A. Soares, M. A. Almeida, C. Marins-Goulart, O. A. Chaves, A. Echevarria, M. C. C. de Oliveira, 'Thiosemicarbazones as inhibitors of tyrosinase enzyme', *Bioorg. Med. Chem. Lett.* **2017**, *27*, 3546-3550.
- [21] K. Hałdys, R. Latajka, 'Thiosemicarbazones with tyrosinase inhibitory activity', *MedChemComm* **2019**, *10*, 378-389.
- [22] M. Yazdani, N. Edraki, R. Badri, M. Khoshneviszadeh, A. Iraj, O. Firuzi, 'Multi-target inhibitors against Alzheimer disease derived from 3-hydrazinyl 1,2,4-triazine scaffold containing pendant phenoxy methyl-1,2,3-triazole: Design, synthesis and biological evaluation', *Bioorg. Chem.* **2019**, *84*, 363-371.
- [23] E. Köksal, I. Gülçin, 'Purification and characterization of peroxidase from cauliflower (*Brassica oleracea* L. var. botrytis) buds', *Protein Pept. Lett.* **2008**, *15*, 320-326.
- [24] H. Gocer, F. Topal, M. Topal, M. Küçük, D. Teke, İ. Gülçin, S. H. Alwasel, C. T. Supuran, 'Acetylcholinesterase and carbonic anhydrase isoenzymes I and II inhibition profiles of taxifolin', *J. Enzyme Inhib. Med. Chem.* **2016**, *31*, 441-447.
- [25] M. Nar, Y. Çetinkaya, İ. Gülçin, A. Menzek, '(3, 4-Dihydroxyphenyl)(2, 3, 4-trihydroxyphenyl) methanone and its derivatives as carbonic anhydrase isoenzymes inhibitors', *J. Enzyme Inhib. Med. Chem.* **2013**, *28*, 402-406.
- [26] İ. Gülçin, 'Antioxidant and antiradical activities of L-carnitine', *Life Sci.* **2006**, *78*, 803-811.
- [27] İ. Gülçin, 'Antioxidant activity of caffeic acid (3, 4-dihydroxycinnamic acid)', *Toxicology* **2006**, *217*, 213-220.
- [28] İ. Gülçin, 'Comparison of in vitro antioxidant and antiradical activities of L-tyrosine and L-Dopa', *Amino acids* **2007**, *32*, 431.
- [29] I. Aouani, K. Lahbib, S. Touil, 'Green synthesis and antioxidant activity of novel γ -cyano- α -hydroxyphosphonate derivatives', *Med. Chem.* **2015**, *11*, 206-213.
- [30] A. Iraj, O. Firuzi, M. Khoshneviszadeh, H. Nadri, N. Edraki, R. Miri, 'Synthesis and structure-activity relationship study of multi-target triazine derivatives as innovative candidates for treatment of Alzheimer's disease', *Bioorg. Chem.* **2018**, *77*, 223-235.
- [31] B. Arabaci, I. Gulcin, S. Alwasel, 'Capsaicin: a potent inhibitor of carbonic anhydrase isoenzymes', *Molecules* **2014**, *19*, 10103-10114.
- [32] N. Öztaskın, P. Taslimi, A. Maraş, İ. Gülçin, S. Göksu, 'Novel antioxidant bromophenols with acetylcholinesterase, butyrylcholinesterase and carbonic anhydrase inhibitory actions', *Bioorg. Chem.* **2017**, *74*, 104-114.

- [33] P. Taslimi, İ. Gülçin, N. Öztaşkın, Y. Cetinkaya, S. Göksu, S. H. Alwasel, C. T. Supuran, 'The effects of some bromophenols on human carbonic anhydrase isoenzymes', *J. Enzyme Inhib. Med. Chem.* **2016**, *31*, 603-607.
- [34] I. Gülçin, Ş. Beydemir, G. Şat, Ö. Küfrevioğlu, 'Evaluation of antioxidant activity of cornelian cherry (*Cornus mas L.*)', *Acta Aliment.* **2005**, *34*, 193-202.
- [35] İ. GÜLÇİN, E. KİREÇCİ, E. AKKEMİK, F. Topal, O. HİSAR, 'Antioxidant and antimicrobial activities of an aquatic plant: Duckweed (*Lemna minor L.*)', *Turk. J. Biol.* **2010**, *34*, 175-188.
- [36] E. Köksal, İ. Gülçin, 'Antioxidant activity of cauliflower (*Brassica oleracea L.*)', *Turk. J. Agric. For.* **2008**, *32*, 65-78.
- [37] A. Irajı, A. Nouri, N. Edraki, S. Pirhadi, M. Khoshneviszadeh, M. Khoshneviszadeh, 'One-pot synthesis of thioxo-tetrahydropyrimidine derivatives as potent β -glucuronidase inhibitor, biological evaluation, molecular docking and molecular dynamics studies', *Bioorg. Med. Chem.* **2020**, 115359.
- [38] A. Irajı, O. Firuzi, M. Khoshneviszadeh, M. Tavakkoli, M. Mahdavi, H. Nadri, N. Edraki, R. Miri, 'Multifunctional iminochromene-2H-carboxamide derivatives containing different aminomethylene triazole with BACE1 inhibitory, neuroprotective and metal chelating properties targeting Alzheimer's disease', *European Journal of Medicinal Chemistry* **2017**, *141*, 690-702.
- [39] N. Edraki, A. Irajı, O. Firuzi, Y. Fattahi, M. Mahdavi, A. Foroumadi, M. Khoshneviszadeh, A. Shafiee, R. Miri, '2-Imino 2H-chromene and 2-(phenylimino) 2H-chromene 3-aryl carboxamide derivatives as novel cytotoxic agents: synthesis, biological assay, and molecular docking study', *Journal of the Iranian Chemical Society* **2016**, *13*, 2163-2171.
- [40] D. Schneidman-Duhovny, O. Dror, Y. Inbar, R. Nussinov, H. J. Wolfson, 'PharmaGist: a webserver for ligand-based pharmacophore detection', *Nucleic Acids Res.* **2008**, *36*, W223-W228.